Synthesis and Spectroscopic Studies of Non-Heme Diiron(III) Species with a Terminal Hydroperoxide Ligand: Models for Hemerythrin

Tadashi J. Mizoguchi,[†] Jane Kuzelka,[†] Bernhard Spingler,[†] Jennifer L. DuBois,[‡] Roman M. Davydov,*[,¶] Britt Hedman,*[,‡,§] Keith O. Hodgson,*[,‡,§] and Stephen J. Lippard*[,†]

Department of Chemistry, Massachusetts Institute of Technology, Cambridge, Massachusetts 02139, Department of Chemistry, Stanford University, Stanford, California 94305, Stanford Synchrotron Radiation Laboratory, SLAC, Stanford University, Stanford, California 94309, and Department of Chemistry, Northwestern University, Evanston, Illinois 60208

Received January 22, 2001

Two compounds, $[Fe_2(\mu\text{-OH})(\mu\text{-Ph}_4\text{DBA})(\text{TMEDA})_2(\text{OTf})]$ (**4**) and $[Fe_2(\mu\text{-OH})(\mu\text{-Ph}_4\text{DBA})(\text{DPE})_2(\text{OTf})]$ (**7**), where Ph_4DBA^{2-} is the dinucleating bis(carboxylate) ligand dibenzofuran-4,6-bis(diphenylacetate), have been prepared as synthetic models for the dioxygen-binding non-heme diiron protein hemerythrin (Hr). X-ray crystallography reveals that, in the solid state, these compounds contain the asymmetric coordination environment found at the diiron center in the reduced form of the protein, deoxyHr. Mössbauer spectra of the models (**4**, $\delta = 1.21(2)$, $\Delta E_Q = 2.87(2)$ mm s^{-1}; **7**, $\delta_{av} = 1.23(1)$, $\Delta E_{Qav} = 2.79(1)$ mm s^{-1}) and deoxyHr ($\delta = 1.19$, $\Delta E_Q = 2.81$ mm s^{-1}) are also in good agreement. Oxygenation of the diiron(II) complexes dissolved in CH_2Cl_2 containing 3 equiv of *N*-MeIm (**4**) or neat EtCN (**7**) at −78 °C affords a red-orange solution with optical bands at 336 nm (7300 M^{-1} cm^{-1}) and 470 nm (2600 M^{-1} cm^{-1}) for **4** and at 334 nm (6400 M^{-1} cm^{-1}) and 484 nm (2350 M^{-1} cm^{-1}) for **7**. These spectra are remarkably similar to that of oxyHr, 330 nm (6800 M^{-1} cm^{-1}) and 500 nm (2200 M^{-1} cm^{-1}). The electron paramagnetic resonance (EPR) spectrum of the cryoreduced, mixed-valence dioxygen adduct of **7** displays properties consistent with a (μ-oxo)diiron(II,III) core. An investigation of **7** and its dioxygen-bound adduct by extended X-ray absorption fine structure (EXAFS) spectroscopy indicates that the oxidized species contains a (μ-oxo)diiron(III) core with iron−ligand distances in agreement with those expected for oxide, carboxylate, and amine/hydroperoxide donor atoms. The analogous cobalt complex $[Co_2(\mu\text{-OH})(\mu\text{-Ph}_4\text{DBA})(\text{TMEDA})_2(\text{OTf})]$ (**6**) was synthesized and structurally characterized, but it was unreactive toward dioxygen.

Introduction

Three proteins bind dioxygen reversibly, hemoglobin (Hb), hemocyanin (Hc), and hemerythrin (Hr).[1] The mononuclear heme−iron site of Hb binds dioxygen end-on, whereas the dicopper active site in Hc binds dioxygen in a μ-η^2:η^2 bidentate fashion.[1] Synthetic models have been prepared that effectively mimic the active site chemistry of both of these proteins.[2−4] Hr, found in certain marine invertebrates, binds dioxygen by forming a monodentate, terminally coordinated hydroperoxide ligand, as depicted in Scheme 1.[1] The active site of Hr contains two non-heme iron(II) centers bridged by two carboxylates from glutamate and aspartate side chains, as well as by a hydroxide ion.[5] The remainder of the coordination spheres are occupied by N-donor imidazole ligands derived from five histidine residues. As a result, deoxyHr has an asymmetric coordination environment with one five-coordinate and one six-coordinate iron center. OxyHr forms when dioxygen binds to the coordinatively unsaturated iron atom with the concomitant two-electron transfer from the iron atoms coupled with proton transfer from the hydroxide ligand to generate a hydroperoxide unit that is hydrogen-bonded to the bridging oxo unit that forms.[5]

Scheme 1

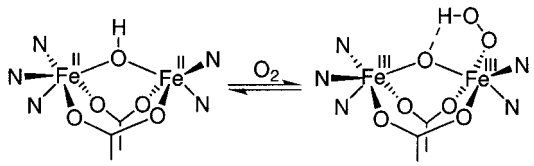

Over the last two decades, there has been significant interest in preparing synthetic models of dioxygen-binding and -activating proteins.[6−10] The earliest compounds prepared include $[(HBpz_3)FeO(CH_3CO_2)_2Fe(HBpz_3)]$, where $HBpz_3$ = hydrotris(1-pyrazolyl)borate,[11] and $[(TACN)_2Fe_2O(CH_3CO_2)_2]I_2$, where TACN = 1,4,7-triazacyclononane.[12] Later work from our laboratory focused on the use of the dicarboxylate ligands based on *m*-xylylenediamine bis(Kemp's triacid) imide, XDK, and compounds such as $[Fe_2(\mu\text{-}O_2CC(CH_3)_3)(\mu\text{-PXDK})(N\text{-MeIm})_2$-

[†] Massachusetts Institute of Technology.
[‡] Department of Chemistry, Stanford University.
[§] Stanford Synchrotron Radiation Laboratory, SLAC, Stanford University.
[¶] Northwestern University.

(1) Lippard, S. J.; Berg, J. M. *Principles of Bioinorganic Chemistry*; University Science: Mill Valley, CA, 1994; pp 284−302.
(2) Momenteau, M.; Reed, C. A. *Chem. Rev.* **1994**, *94*, 659−698.
(3) Kitajima, N.; Moro-oka, Y. *Chem. Rev.* **1994**, *94*, 737−757.
(4) Tolman, W. B. *Acc. Chem. Res.* **1997**, *30*, 227−237.
(5) Stenkamp, R. E. *Chem. Rev.* **1994**, *94*, 715−726.
(6) Fontecave, M.; Ménage, S.; Duboc-Toia, C. *Coord. Chem. Rev.* **1998**, *178−180*, 1555−1572.
(7) Que, L., Jr. *J. Chem. Soc., Dalton Trans.* **1997**, 3933−3940.
(8) Feig, A. L.; Lippard, S. J. *Chem. Rev.* **1994**, *94*, 759−805.
(9) Kurtz, D. M., Jr. *Chem. Rev.* **1990**, *90*, 585−606.
(10) Lippard, S. J. *Angew. Chem., Int. Ed. Engl.* **1988**, *27*, 344−361.
(11) Armstrong, W. H.; Lippard, S. J. *J. Am. Chem. Soc.* **1983**, *105*, 4837−4838.
(12) Wieghardt, K.; Pohl, K.; Gebert, W. *Angew. Chem., Int. Ed. Engl.* **1983**, *22*, 727.

10.1021/ic010076b CCC: $20.00
Published on Web 07/21/2001

$(O_2CC(CH_3)_3)$], where PXDK = *m*-xylylenediamine bis(propyl Kemp's triacid) imide, were prepared.[13] The chemistry of these and other diiron complexes with dioxygen does not mimic that of the Hr active site, however, owing to difficulties such as the lack of an open coordination site for O_2 binding or reaction with dioxygen to form μ-1,2-peroxo species.

Previously, we communicated the first synthetic example of a diiron complex that mimics the chemical reactivity of the Hr active site.[14] In the presence of 3 equiv of *N*-MeIm, [Fe_2(μ-OH)(μ-Ph_4DBA)(TMEDA)$_2$(OTf)] (**4**) reacts with O_2 at −78 °C to generate a species having an optical spectrum similar to that of oxyHr.[15] On the basis of this similarity, as well as Mössbauer and resonance Raman spectroscopic results, we proposed the formation of a monodentate, terminally coordinated hydroperoxide ligand, as in Hr. We now wish to report the detailed preparation and spectroscopic investigation of a related complex, [Fe_2(μ-OH)(μ-Ph_4DBA)(DPE)$_2$(OTf)], where DPE is dipyrrolidinoethane, that is more stable under similar oxygenation conditions. Studies of the hydroperoxide derivatives of the two species by Mössbauer, resonance Raman, electron paramagnetic resonance (EPR), electron nuclear double resonance (ENDOR), and extended X-ray absorption fine structure (EXAFS) spectroscopy are described. The instability of the dioxygen adducts at low temperature precluded their isolation in the solid state for characterization by X-ray methods. Our interest in obtaining the structure of such an adduct led us to prepare the cobalt analog [Co_2(μ-OH)(μ-Ph_4DBA)(TMEDA)$_2$(OTf)] and study its oxygenation chemistry, because the kinetic inertness of Co(III) can stabilize superoxo and peroxo adducts.[16−18]

Experimental Section

General. Solvents were purified following standard procedures. *N*,*N*,*N*′,*N*′-tetramethylethylenediamine (TMEDA) and DPE[19] were distilled over CaH_2. Dibenzofuran (90% from Aldrich) was recrystallized from a mixture of EtOH and H_2O prior to use. $Fe(OTf)_2$·$2CH_3CN$, where OTf = triflate, was synthesized according to a literature procedure.[20] Compounds **4** and **5** were prepared as described previously.[14] All other reagents were purchased from commercial sources and used as received unless otherwise noted. Air-sensitive manipulations were performed under nitrogen in a Vacuum Atmospheres glovebox.

4,6-Bis(hydroxydiphenylmethyl)dibenzofuran (1). To a solution of dibenzofuran (10.0 g, 59.5 mmol) and TMEDA (29 mL, 192 mmol) in dry hexanes (90 mL) was added 1.6 M *n*-butyllithium in hexanes (122 mL, 195 mmol) at room temperature. The resulting mixture was allowed to stir for several minutes, after which time it was refluxed for 1 h. After the mixture cooled to room temperature, powdered benzophenone (35 g, 192 mmol) was added at once with rapid stirring. The mixture was stirred for several hours before the reaction was quenched by the careful addition of H_2O (60 mL). This mixture was extracted with CH_2Cl_2 (1 L total), and the organic layer was dried over $MgSO_4$ and filtered. Rotary evaporation of the filtrate afforded a yellow oil from which a precipitate deposited upon standing. The solid was collected and washed successively with hexanes, Et_2O, and 1:1 CH_2Cl_2/hexanes to yield **1** as an off-white solid that was dried under vacuum (14.2 g, 45%). ^{1}H NMR (250 MHz, CD_2Cl_2): δ 7.92 d (J = 31 Hz, 2H), 7.4−7.1 m (22H), 6.85 d (J = 30 Hz, 2H). IR (cm^{-1}, KBr pellet): 3567, 3534, 1597, 1579, 1489, 1444, 1426, 1408, 1334, 1297, 1186, 1030, 1001, 986, 846, 779, 770, 750, 742, 701, 634. Anal. Calcd for $C_{38}H_{29}O_{3.5}$ (**1**·0.5H_2O): C, 84.27; H, 5.40. Found: C, 84.48; H, 5.39.

4,6-Bis(diphenylmethyl)dibenzofuran (2). To a solution of **1** (7.0 g, 13 mmol) in dry CH_2Cl_2 (100 mL) was added triethylsilane (4.9 mL, 31 mmol). After this solution was cooled in an ice bath, BF_3·Et_2O (4.6 mL, 37 mmol) was added with rapid stirring. The resulting dark red solution was stirred for 15 min at 0 °C followed by another 1 h at room temperature. The reaction was quenched by addition of saturated Na_2CO_3 (35 mL), and the organic product was extracted with 3 × 50 mL of Et_2O. The Et_2O layer was dried over $MgSO_4$ and filtered. Rotary evaporation of the filtrate and subsequent drying under vacuum yielded an off-white solid. This material was washed with hexanes to afford **2** as a white powder (5.5 g, 83%). ^{1}H NMR (250 MHz, $CDCl_3$): δ 7.83 d (J = 30 Hz, 2H), 7.3−7.0 m (24H), 5.93 s (2H). IR (cm^{-1}, KBr pellet): 3082, 3058, 3024, 3001, 1598, 1584, 1494, 1447, 1431, 1416, 1193, 1079, 1056, 1031, 785, 767, 742, 700, 626. Anal. Calcd for $C_{38}H_{28}O$: C, 91.17; H, 5.64. Found: C, 90.67; H, 5.57.

Dibenzofuran-4,6-bis(diphenylacetic acid) (3, H_2Ph_4DBA). To an ice-cold, stirred solution of **2** (5.30 g, 10.6 mmol) in dry THF (80 mL) was added 1.6 M *n*-butyllithium in hexanes (19.8 mL, 31.7 mmol). The resulting dark green solution was stirred at 0 °C for 1 h. Dry CO_2(g) was passed over the reaction mixture, leading to a color change to light yellow within 5 min. After the solution was stirred for 30 min under a CO_2 atmosphere, the reaction was quenched by the addition of 1 M HCl in THF (66 mL). Rotary evaporation of the resulting mixture yielded a yellow solid that was subsequently stirred overnight in a 1:1 mixture of H_2O and Et_2O (120 mL total). The crude product was filtered and then washed with H_2O and Et_2O to yield **3** as a white solid (3.7 g, 59%). ^{1}H NMR (250 MHz, DMSO-d_6): δ 8.01 d (J = 28 Hz, 2H), 7.3−7.1 m (22H), 6.98 d (J = 28 Hz, 2H). IR (cm^{-1}, KBr pellet): 1748, 1724, 1691, 1597, 1582, 1496, 1446, 1425, 1409, 1236, 1189, 1067, 1036, 850, 778, 741, 694, 653. Anal. Calcd for $C_{40}H_{28}O_5$: C, 81.62; H, 4.79. Found: C, 81.81; H, 4.81.

[Co_2(μ-OH)(μ-Ph_4DBA)(TMEDA)$_2$(OTf)] (6). To a stirred solution of $CoBr_2$ (208 mg, 950 μmol) and TMEDA (1.4 mL, 9.5 mmol) in acetonitrile (5 mL) was added dropwise a solution of Tl(OTf) (671 mg, 1.9 mmol) in acetonitrile (10 mL). Immediate precipitation of TlBr occurred, and the suspension was vigorously stirred for 10 min. The mixture was filtered through a glass filter, and to the resulting orange-pink solution was added a solution of diacid **3** (280 mg, 475 μmol) and NEt_3 (195 μL, 1.4 mmol) in THF (10 mL). After 20 min of stirring, H_2O (12.8 μL, 713 μmol) was added to the purple-pink solution. A fine white precipitate formed over 30 min, and the suspension was filtered through a plug of Celite. The clear filtrate was evaporated to dryness under vacuum. Recrystallization from THF/pentane yielded **6** (327 mg, 62%). X-ray quality crystals of **6**·$PhCH_3$ were grown from a solution of CH_2Cl_2/toluene/hexanes. IR (cm^{-1}, KBr pellet): 3087, 3058, 2889, 2839, 1630, 1495, 1469, 1442, 1374, 1291, 1246, 1164, 1033, 801, 767, 740, 726, 696, 636, 516. Anal. Calcd for $C_{53}H_{59}N_4O_9F_3SCo_2$: C, 57.71; H, 5.39; N, 5.08. Found: C, 57.92; H, 5.62; N, 4.97.

[Fe_2(μ-OH)(μ-Ph_4DBA)(DPE)$_2$(OTf)] (7). To a stirred solution of $Fe(OTf)_2$·$2CH_3CN$ (405 mg, 1.02 mmol) and DPE (156 mg, 0.93 mmol) in acetonitrile (5 mL) was added dropwise a solution of diacid **3** (274 mg, 470 μmol) and Et_3N (194 μL, 1.4 mmol) in THF (10 mL). To the resulting pale yellow solution was added water (13 μL, 720 μmol) with vigorous stirring. After several minutes, the solution turned green with concomitant formation of a green precipitate. This mixture was filtered through a plug of Celite, and the clear filtrate was evaporated to dryness under vacuum. A solution of 1:1 CH_3CN/Et_2O was added to the resulting solid, and the suspension was placed in a −20 °C freezer overnight to yield a gray solid. The brown supernatant was removed by pipet, and the solid was washed with a cold mixture of 1:1 CH_3CN/Et_2O to yield **7** in >90% yield. The off-white solid was then resuspended in THF (15 mL), and the pale yellow mixture was passed

(13) Herold, S.; Lippard, S. J. *J. Am. Chem. Soc.* **1997**, *119*, 145−156.
(14) Mizoguchi, T. J.; Lippard, S. J. *J. Am. Chem. Soc.* **1998**, *120*, 11022−11023.
(15) Garbett, K.; Darnall, D. W.; Klotz, I. M.; Williams, R. J. P. *Arch. Biochem. Biophys.* **1969**, *135*, 419−434.
(16) Suzuki, M.; Ueda, I.; Kanatomi, H.; Murase, I. *Chem. Lett.* **1983**, 185−188.
(17) Ookubo, T.; Sugimoto, H.; Nagayama, T.; Masuda, H.; Sato, T.; Tanaka, K.; Maeda, Y.; Ōkawa, H.; Hayashi, Y.; Uehara, A.; Suzuki, M. *J. Am. Chem. Soc.* **1996**, *118*, 701−702.
(18) Bianchini, C.; Zoellner, R. W. *Adv. Inorg. Chem.* **1997**, *44*, 263−339.
(19) Remenar, J. F.; Lucht, B. L.; Collum, D. B. *J. Am. Chem. Soc.* **1997**, *119*, 5567−5572.
(20) Diebold, A.; Elbouadili, A.; Hagen, K. S. *Inorg. Chem.* **2000**, *39*, 3915−3923.

Table 1. Summary of X-ray Crystallographic Data

	6·$PhCH_3$	**7**·1.5$PhCH_3$	**8**·0.5THF·0.25C_5H_{12}
formula	$C_{60}H_{67}N_4O_9F_3SCo_2$	$C_{71.5}H_{79}N_4O_9F_3SFe_2$	$C_{62.25}H_{73}N_4O_{12.5}F_6S_2Fe_2$
fw	1195.10	1339.15	1403.13
space group	$P2_1/n$	$P\bar{1}$	$P2_1/c$
a, Å	12.1202(4)	12.1852(2)	13.3723(3)
b, Å	16.3151(5)	14.6388(2)	15.4576(4)
c, Å	29.2527(9)	19.7878(3)	33.6514(1)
α, deg		97.106(1)	
β, deg	99.270(1)	96.290(1)	99.732(1)
γ, deg		111.294(1)	
V, Å^3	5709.0(3)	3217.57(8)	6855.8(2)
Z	4	2	4
T, °C	−85	−85	−85
ρ_{calcd}, g cm^{-3}	1.390	1.382	1.353
μ(Mo Kα), mm^{-1}	0.687	0.554	0.562
2θ range, deg	3−57	4−57	3−57
total no. of data	35497	20371	42671
no. of unique data	13261	14209	15982
observed data[a]	9327	11469	9368
no. of params	712	783	914
R^b	0.0505	0.0456	0.0923
wR2[c]	0.1204	0.1220	0.2424
max, min peaks, e Å^{-3}	1.542, −0.573	1.092, −0.604	1.418, −0.781

[a] Observation criterion: $I > 2\sigma(I)$. [b] $R = \sum||F_o - F_c||/\sum|F_o|$. [c] wR2 = $\{\sum[w(F_o^2 - F_c^2)^2]/\sum[w(F_o^2)^2]\}^{1/2}$.

through a plug of Celite. Exposure of this solution to pentane vapor diffusion resulted in the isolation of a crystalline solid. Single crystals suitable for X-ray diffraction study formed from a solution of toluene and pentane. IR (cm^{-1}, KBr pellet): 3059, 2972, 2877, 1629, 1592, 1491, 1459, 1443, 1421, 1373, 1293, 1272, 1237, 1222, 1114, 1064, 1031, 965, 936, 766, 726, 699, 636. Anal. Calcd for $C_{61}H_{67}N_4O_9F_3SFe_2$: C, 61.01; H, 5.62; N, 4.67. Found: C, 60.51; H, 5.94; N, 4.45.

[Fe$_2$(μ-O)(μ-Ph$_4$DBA)(DPE)$_2$(OTf)$_2$] (8). To a solution of **7** (91 mg, 76 μmol) and NEt_3 (11 μL, 76 μmol) in THF (5 mL) was added dropwise a solution of AgOTf (39 mg, 152 μmol) in THF (5 mL). The resultant brown-red suspension was stirred for 2.5 h. The mixture was filtered through a plug of Celite, and the clear filtrate was evaporated to dryness under vacuum. Recrystallization from CH_2Cl_2/THF/pentane/hexanes resulted in the isolation of **8**·0.5THF·0.25C_5H_{12} as a crystalline solid (90 mg, 87%) that was suitable for X-ray diffraction. IR (cm^{-1}, Nujol mull): 1571, 1311 1235, 1217, 1173, 1029, 966, 942, 848, 773, 736, 725, 634. Anal. Calcd for $C_{62}H_{66}N_4O_{12}F_6S_2Fe_2$: C, 55.20; H, 4.93; N, 4.15. Found: C, 55.38; H, 4.61; N, 3.78.

Generation of Dioxygen-Bound Adducts of 4 and 7. In a typical reaction, compound **4** or **7** was dissolved in CH_2Cl_2 containing 3 equiv of *N*-MeIm. The resulting solution was transferred to a vessel that was subsequently sealed with a rubber septum and cooled to −78 °C in a dry ice/acetone bath. Dioxygen, passed through a column of Drierite, was bubbled directly into the cold solution via a stainless steel needle for 30−60 s. The solution immediately turned red-orange, indicating the formation of an adduct.

Physical Measurements. ^{1}H NMR spectra were recorded with a Bruker AC-250 spectrometer. Optical spectra were recorded on a Hewlett-Packard 8452A diode-array spectrophotometer; low-temperature experiments were executed by using a custom-made quartz cuvette fused onto a vacuum-jacketed Dewar. FT-IR spectra were recorded on a Bio-Rad FTS 135 spectrometer.

X-ray Crystallography. Crystallographic information for **6**·$PhCH_3$, **7**·1.5$PhCH_3$, and **8**·0.5THF·0.25C_5H_{12} is provided in Table 1. Crystals were mounted in Paratone N oil on the ends of glass capillaries and frozen into place under a low-temperature nitrogen cold stream. Data were collected on a Bruker (formerly Siemens) SMART/CCD X-ray diffractometer, running the SMART software package,[21] with Mo Kα radiation (λ = 0.710 73 Å). Details of the data collection and reduction protocols are described elsewhere.[22] The structures were solved by direct methods and refined on F^2 by using the SHELXTL program package.[23] The possibility of higher symmetry was checked by the program PLATON.[24] All non-hydrogen atoms were located and their positions refined by least-squares cycles and Fourier syntheses. Hydrogen atoms were assigned idealized positions and given a thermal parameter that was 1.2 times the thermal parameter of the carbon atom to which each was attached. Empirical absorption corrections were applied by using the SADABS program.[25]

For compound **6**, the thermal ellipsoid for O101 was significantly elongated, but we were unable to account satisfactorily for this feature either by disorder or by the introduction of an alternative bridging ligand in the model. In the structure of **7**, the lattice contains 1.5 molecules of toluene. One molecule was modeled over two positions, each with 50% occupancy, whereas the other solvent molecule is located on a special position with the methyl substituent disordered in opposite directions. In the structure of **8**, one coordinated triflate ligand was disordered and modeled over two positions, with occupancies of 58% and 42%. Appropriate restraints were placed on both the THF molecule and bound triflate.

Mössbauer Spectroscopy. Solid samples were prepared by suspending powdered material (∼0.04 mmol) in Apiezon N grease, and frozen solutions were made by flash-freezing the solutions (∼50 mM) in liquid N_2. The O_2-adduct was prepared by adding 60 mL of dry dioxygen to a solution of **4** or **7** in a nylon sample holder at −78 °C via a gastight syringe. Mössbauer spectra were recorded in the MIT Department of Chemistry Instrumentation Facility at 4.2 K with a ^{57}Co source in a Rh matrix at room temperature and fit to Lorentzian line shapes by using the WMOSS plot and fit program.[26] Isomer shifts were referenced to natural abundance Fe at room temperature.

Resonance Raman Spectroscopy. Raman data were obtained with a Coherent Innova 90 Kr^+ laser with an excitation wavelength of 514.5 nm and 90 mW of power. A 0.6-m single monochromator (1200 grooves/nm grating), with an entrance slit of 100 μm, and a liquid-nitrogen-cooled CCD detector (Princeton Instruments) were used in a standard backscattering configuration. A holographic notch filter (Kaiser Optical Systems) was used to attenuate Rayleigh scattering. Spectra of the O_2-adduct formed by reaction of compound **7** (∼13 mM) and a

(21) *SMART*, version 4.0; Siemens Industrial Automation, Inc.: Madison, WI, 1995.
(22) Feig, A. L.; Bautista, M. T.; Lippard, S. J. *Inorg. Chem.* **1996**, *35*, 6892−6898.
(23) *SHELXTL: Structure Analysis Program*, version 5.0; Siemens Industrial Automation, Inc.: Madison, WI, 1995.
(24) Spek, A. L. *PLATON, A Multipurpose Crystallographic Tool*; Utrecht University: Utrecht, The Netherlands, 1998.
(25) Sheldrick, G. M. *SADABS: Area-Detector Absorption Correction*; University of Göttingen: Göttingen, Germany, 1996.
(26) Kent, T. A. *WMOSS: Mössbauer Spectral Analysis Software*, version 2.5; WEB Research Co.: Minneapolis, MN, 1998.

statistical mixture of $^{16}O_2$ and $^{18}O_2$ (Cambridge Isotope Laboratories) were collected in CH_2Cl_2 solution containing 1% CH_3CN at −78 °C with the same low-temperature Dewar used to obtain UV−vis spectra. A total of 600 scans, each with a 1-s exposure time, were collected for the sample. Raman shifts were calibrated with CH_2Cl_2 as an internal standard. The data were processed by using CSMA software (Princeton Instruments, version 2.4A) on a Gateway 2000 computer, and the resulting ASCII files were processed with the software package Kaleidagraph (Abelbeck Software).

Cryogenic Reduction. The O_2-adduct of complex **7** was prepared by gently bubbling dioxygen into 60 μL of a 5 mM solution of **7** in 2:1 2-MeTHF/EtCN at −78 °C in 3-mm i.d. quartz tubes. The samples were flash-frozen in liquid nitrogen and irradiated by γ-rays generated from a ^{60}Co source as described previously.[27,28]

EPR and ENDOR Spectroscopy. The 35 GHz EPR and ENDOR spectra were obtained on the spectrometer described elsewhere.[29,30]

EXAFS Spectroscopy. Samples of **7** and its dioxygen adduct were prepared as EtCN solutions in 1-mm-thick Lexan cells with X-ray transparent Mylar windows and then flash frozen in liquid nitrogen. X-ray absorption spectra (XAS) were measured on unfocused wiggler beamline 7-3 at the Stanford Synchrotron Radiation Laboratory (SSRL), with the ring operating at 3 GeV and 50−100 mA. Samples were maintained at 10 K inside an Oxford Instruments CF-1208 liquid helium continuous flow cryostat. A Si(220) double-crystal monochromator was used, detuned 50% at 7987 eV in order to minimize contamination of the radiation by higher harmonics. Vertical 1-mm pre-monochromator slits were used to define the beam size, minimizing beam divergence and allowing for an energy resolution of ≤1−1.4 eV at the Fe K-edge.[31] K-edge and EXAFS data were measured over the energy range 6786−7987 eV for all samples. Spectra were collected in fluorescence mode, using a Lytle detector, an ion chamber equipped with a manganese filter and Soller slits. The spectrum of Fe foil was collected concomitantly, allowing for internal energy calibration of the spectra, and the first inflection point energy for the Fe foil spectrum was set to 7111.2 eV. Reproducibility in the determination of edge position was less than 0.2 eV. Twelve scans over the complete energy range were averaged for each sample. Although EXAFS data were collected to $k = 15$ Å^{-1}, spectra were truncated at 13 Å^{-1} due to noise in the data at higher values of k.

For each spectrum, a smooth second-order polynomial was fit to the preedge region and then extrapolated and subtracted from the data. A three-segment spline (polynomial curves of orders 2, 3, and 3) was fit and subtracted from the EXAFS region; the data were normalized at 7130 eV, using the SPLINE program (written by Dr. Paul Ellis). EXAFS data were then k^3-weighted, where the photoelectron wave vector $k = [2m_e/(E - E_0)/(h/2\pi)^2]^{1/2}$, E is energy, E_0 is the energy of onset of the EXAFS, and m_e is the mass of an electron. Phase and amplitude functions calculated by FEFF 6.0[32] were used in creating a simulated EXAFS spectrum, which was adjusted by a least-squares fitting process to match the data (using the EXAFSPAK programs by Dr. G. N. George, SSRL, which utilize the public domain MINPAK fitting library).[33] Absorber−scatterer distances and Debye−Waller factors were varied for each equivalent set of backscattering atoms, and coordination numbers (N_s) were kept constant according to the known crystal structure of compound **7**. Other parameters included in the fits were E_0 and S_0^2. E_0 was allowed to vary within ranges defined by fits to similar crystallographically characterized diiron(II) and diiron(III) complexes. S_0^2 was fixed at 0.9. Fits were constructed in a building-up process, where components to the fit were included on the basis of visual improvement to the EXAFS fit and reduction in a goodness-of-fit parameter R, where $R = R^2/[(2\Delta k \Delta R/\pi) - \text{no. variables in fit}]$, $R = [\sum k^6(\chi_{obs} - \chi_{calc})^2/N]^{1/2}$ and $N =$ the number of points in the EXAFS spectrum.[34]

Chart 1

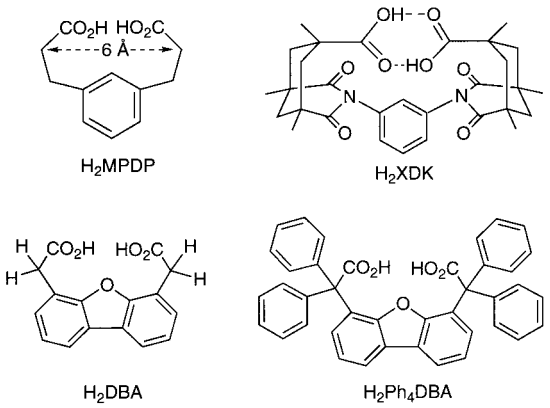

Results and Discussion

Ligand Design. Our interest in preparing small-molecule models of non-heme diiron proteins and enzymes led us to utilize the dinucleating dicarboxylate ligands H_2MPDP, *m*-phenylenedipropionicacid,[35] and H_2XDK, *m*-xylylenediamine bis(Kemp's triacid) imide,[36] both of which are shown in Chart 1. The H_2MPDP ligand was designed to have a 6 Å span between the β-methylene carbon atoms in order to match the distance between the acetate methyl carbon atoms of [(HBpz$_3$)Fe(μ-O)(μ-O$_2$CCH$_3$)$_2$Fe(HBpz$_3$)],[37] a complex that is a good structural and spectroscopic model for metHr, the chemically oxidized diiron(III) form of Hr. This dicarboxylate ligand forms diiron compounds containing bidentate nitrogen donors and terminal monodentate ligands, the structural motif of which was previously inaccessible by the use of monoacid ligands.[38] These diferric compounds, however, are air-stable and hence did not allow us to prepare a functional model of the protein Hr. The use of the XDK ligand system resulted in the isolation of a series of dioxygen-binding model compounds.[13,39] Reaction of (μ-XDK)diiron(II) compounds with dioxygen generates μ-1,2-peroxo species and thus does not mimic the oxidation chemistry of Hr. In addition, despite extensive efforts, a (μ-hydroxo)-(μ-XDK)diiron(II) complex that would allow us access to important structures such as those that model the core of deoxyHr has yet to be realized.[13]

These apparent shortcomings of the XDK ligand system prompted us to design a new dinucleating dicarboxylate ligand so that we might address functionally relevant aspects of Hr. In particular, we desired the nearly orthogonal orientation of the two carboxylate groups that bridge the two metal centers, a geometric feature incompatible with the convergent nature of

(27) Mizoguchi, T. J.; Davydov, R. M.; Lippard, S. J. *Inorg. Chem.* **1999**, *38*, 4098−4103.
(28) Davydov, R. M.; Smieja, J.; Dikanov, S. A.; Zang, Y.; Que, L., Jr.; Bowman, M. K. *J. Biol. Inorg. Chem.* **1999**, *49*, 292−301.
(29) DeRose, V. J.; Liu, K. E.; Lippard, S. J.; Hoffman, B. M. *J. Am. Chem. Soc.* **1996**, *118*, 121−134.
(30) Werst, M. M.; Davoust, C. E.; Hoffman, B. M. *J. Am. Chem. Soc.* **1991**, *113*, 1533−1538.
(31) Lytle, F. W. In *Applications of Synchrotron Radiation*; Winick, H., Xiam, D., Ye, M.-H., Huang, T., Eds.; Gordon and Breach Science Publishers: New York, 1989; Vol. 4, pp 135−223.
(32) Mustre de Leon, J.; Rehr, J. J.; Zabinsky, S. I.; Albers, R. C. *Phys. Rev. B* **1991**, *44*, 4146−4156.
(33) More, J. J.; Garbow, B. S.; Hillstrom, K. E. *User Guide for MINPACK-1*; Applied Mathematics Division Report ANL-80-74; Argonne National Laboratory: Argonne, IL, 1980.
(34) Lytle, F. W.; Sayers, D. E.; Stern, E. A. *Phys. B* **1989**, *158*, 701−722.
(35) Schimelpfenig, C. W. *J. Org. Chem.* **1975**, *40*, 1493−1494.
(36) Rebek, J., Jr.; Marshall, L.; Wolak, R.; Parris, K.; Killoran, M.; Askew, B.; Nemeth, D.; Islam, N. *J. Am. Chem. Soc.* **1985**, *107*, 7476−7481.
(37) Armstrong, W. H.; Spool, A.; Papaefthymiou, G. C.; Frankel, R. B.; Lippard, S. J. *J. Am. Chem. Soc.* **1984**, *106*, 3653−3667.
(38) Beer, R. H.; Tolman, W. B.; Bott, S. G.; Lippard, S. J. *Inorg. Chem.* **1989**, *28*, 4557−4559.
(39) LeCloux, D. D.; Barrios, A. M.; Mizoguchi, T. J.; Lippard, S. J. *J. Am. Chem. Soc.* **1998**, *120*, 9001−9014.

Scheme 2

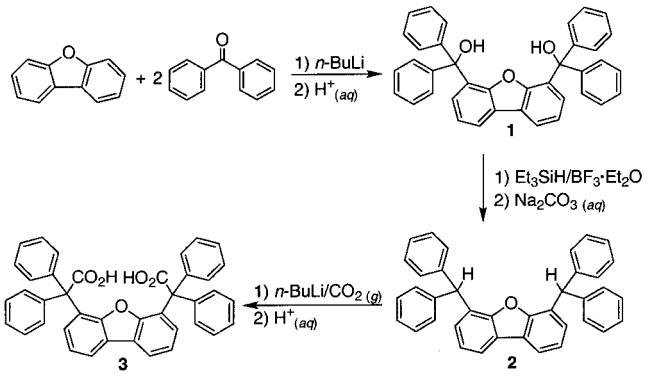

the carboxylic acid groups in H_2XDK. Through the use of computer modeling, we found that the structure of dibenzofuran-4,6-diacetic acid (H_2DBA) could be oriented to present an orthogonal pair of properly spaced carboxylate groups. The replacement of all four methylene hydrogens with phenyl groups to afford dibenzofuran-4,6-bis(diphenylacetic acid) (H_2Ph_4DBA) rendered a molecule designed to preorganize the carboxylates in the appropriate fashion through nonbonding interactions and to promote the crystallinity and solubility of compounds containing this ligand.

Preparation of the Dinucleating Ligand H_2Ph_4DBA. The compound H_2Ph_4DBA (**3**) was prepared by a three-step procedure, outlined in Scheme 2. First, we generated the dibenzofuran dianion to which was added benzophenone. Acidic workup resulted in the crystalline product **1**. Reduction of **1** with triethylsilane/BF_3·Et_2O produced compound **2** in high yield.[40] Double deprotonation of **2** followed by addition of CO_2(g) and acidic workup generated the diacid **3** in moderate yield.

Preparation of (μ-Hydroxo)(μ-Ph_4DBA)diiron(II) Compounds. The combination of $Fe(OTf)_2$·$2CH_2CN$, Ph_4DBA^{2-}, OH^-, and TMEDA (for **4**) or DPE (for **7**) results in the self-assembly of [Fe_2(μ-OH)(μ-Ph_4DBA)(TMEDA)$_2$(OTf)] (**4**)[14] and [Fe_2(μ-OH)(μ-Ph_4DBA)(DPE)$_2$(OTf)] (**7**) in good yield. The purity of these compounds requires the crude solid to be washed with cold CH_3CN (for **4**) or cold 1:1 CH_3CN/Et_2O (for **7**). In the solid state, **4** and **7** have asymmetric diiron centers. The triflate ligand of **4** can be replaced by a molecule of acetonitrile. Upon addition of $NaBPh_4$ and recrystallization of the product from $CH_2Cl_2/CH_3CN/Et_2O$, [Fe_2(μ-OH)(μ-Ph_4DBA)(TMEDA)$_2$-(CH_3CN)]BPh_4 (**5**) is obtained.[14] The cation retains the asymmetric coordination environment of **4**. Sketches of compounds **4**−**8** are presented in Chart 2.

Synthesis of an Analogous Dicobalt Complex. The in situ preparation of $Co(OTf)_2$ by reacting $CoBr_2$ with Tl(OTf) was followed by addition of TMEDA, Ph_4DBA^{2-}, and hydroxide ion to generate [Co_2(μ-OH)(μ-Ph_4DBA)(TMEDA)$_2$(OTf)] (**6**). Whereas the preparation of **4** required only 2 equiv of TMEDA for each equivalent of dinucleating ligand, 20 equiv were needed to form the neutral dicobalt complex **6**. The addition of smaller amounts of TMEDA resulted in the isolation of a trinuclear cobalt complex, [Co_3(μ-OH)$_2$(μ-Ph_4DBA)$_2$(TMEDA)$_2$(Tl(OTf))$_2$], a sketch of which is depicted in Figure 1.[41] This linear arrangement of metal centers is not uncommon and, once formed, is not facile to disassemble.[42] The asymmetric coordination environment of the metal ions in **4** is preserved in **6**.

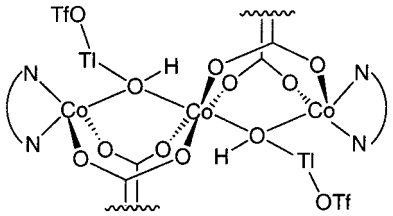

Figure 1. Schematic representation of the complex [Co_3(μ-OH)$_2$(μ-Ph_4DBA)$_2$(TMEDA)$_2$(Tl(OTf))$_2$].

Chart 2

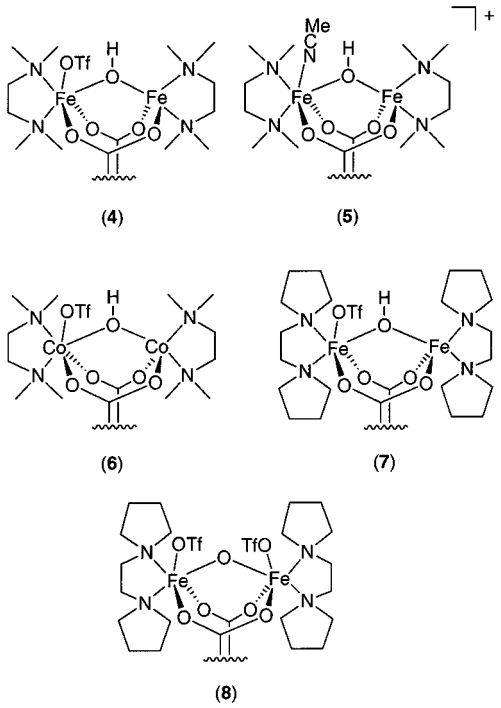

Chemical Oxidation To Form a (μ-Oxo)diiron(III) Compound. The treatment of a solution of **7** in THF with 2 equiv of AgOTf proved sufficient to oxidize each iron(II) center by one electron. Triethylamine was added to deprotonate the bridging hydroxide in **7** to generate the (μ-oxo)diiron(III) core. The neutral complex **8** has a symmetrical coordination geometry that contrasts with that of the asymmetric (μ-hydroxo)bis(μ-carboxylato)dimetal(II) complexes and reflects the greater preference of Fe(III) to be six-coordinate.

Crystal Structures of Dinuclear Complexes Containing the Nitrogen-Donor Ligand TMEDA. The disorder of the two TMEDA ligands and the lattice solvent molecules prevented us from obtaining a completely refined structure of **4**.[14] Replacement of the bound triflate ligand by a molecule of acetonitrile, however, generates a cation that was crystallized as the tetraphenylborate salt, the structure of which was determined and reported.[14] An ORTEP diagram of this compound (**5**) is shown in Figure 2.

X-ray quality crystals of **6**·$PhCH_3$ were grown by vapor diffusion of hexanes into a solution of the compound in CH_2Cl_2 and toluene. The structure of **6** is shown in Figure 3, and selected bond lengths and angles are listed in Table 2. The two metal centers are bridged by the two carboxylate groups of the Ph_4DBA^{2-} ligand as well as by a hydroxide ion. Each cobalt atom is further ligated by the two nitrogen atoms of TMEDA,

(40) Orfanopoulos, M.; Smonou, I. *Synth. Commun.* **1988**, *18*, 833−839.

(41) X-ray data for [Co_3(μ-OH)$_2$(μ-Ph_4DBA)$_2$(TMEDA)$_2$(Tl(OTf))$_2$]·$3CH_2Cl_2$·CH_3CN: triclinic, $P\bar{1}$, a = 14.777(5) Å, b = 18.055(5) Å, c = 19.734(5) Å, α = 83.222(5)°, β = 89.442(5)°, γ = 85.426(5)°, V = 5212(3) Å^3 at −85 °C with Z = 2; R1 = 5.30% ($I > 2\sigma(I)$).

(42) Rardin, R. L.; Tolman, W. B.; Lippard, S. J. *New J. Chem.* **1991**, *15*, 417−430.

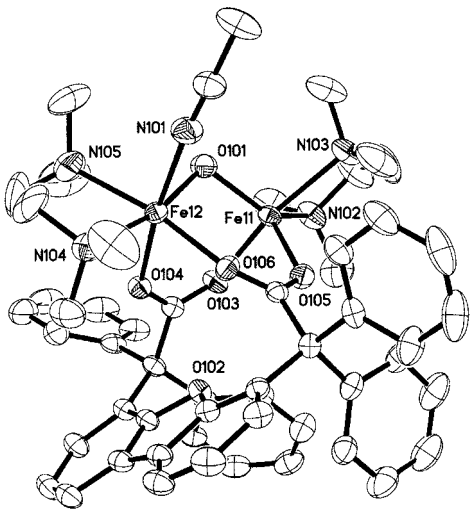

Figure 2. ORTEP diagram of $[Fe_2(\mu\text{-OH})(\mu\text{-Ph}_4\text{DBA})(\text{TMEDA})_2(\text{CH}_3\text{CN})]^+$ (**5**) showing 50% probability thermal ellipsoids for all non-hydrogen atoms.[14]

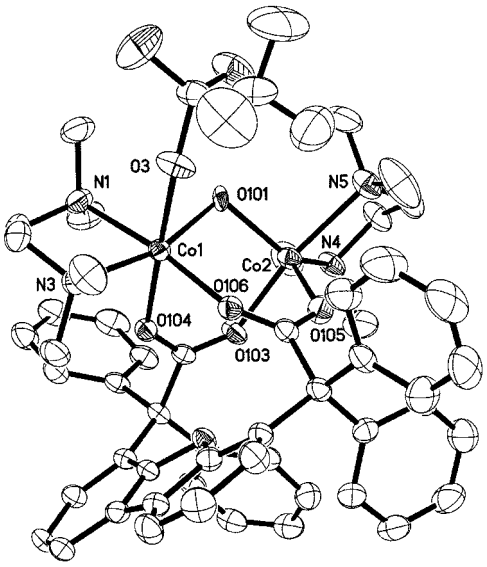

Figure 3. ORTEP diagram of $[Co_2(\mu\text{-OH})(\mu\text{-Ph}_4\text{DBA})(\text{TMEDA})_2(\text{OTf})]$ (**6**) showing 50% probability thermal ellipsoids for all non-hydrogen atoms.

and the coordination sphere of Co(1) is completed by a terminally bound triflate molecule. The asymmetric environment of **6** results in a pseudooctahedral environment at Co(1) and a distorted trigonal bipyramidal stereochemistry at Co(2). The Co···Co separation is 3.2617(5) Å, and the Co−O(H)−Co bond angle is 104.14(11)°. The Co−O(H) distances are 1.9876(19) and 2.146(3) Å; the six-coordinate cobalt atom has the longer Co−O(H) bond. The carboxylate groups are bound with Co−O bond lengths ranging from 1.988(2) to 2.1220(19) Å. The two TMEDA ligands are tilted away from each another, presumably a result of their different coordination environments. The Co−N bond lengths of the six-coordinate metal center average to 2.221(1) Å, and the corresponding distances for the coordinatively unsaturated cobalt atom are, on average, 2.197(2) Å, with the shorter Co−N bonds being those located trans to the bridging hydroxide. The coordinatively saturated Co(1) center has a $Co-O_{OTf}$ bond length of 2.257(2) Å. As in complexes **4** and **5**, the dibenzofuran unit is canted toward the six-coordinate metal center. The Ph_4DBA^{2-} ligand was designed to orient the carboxylate groups orthogonal to one another, in direct contrast to the convergent nature of the carboxylates of XDK. The success of this strategy is evident from the dihedral angle, defined by the angle between the two O−C−O carboxylate planes, of 68.17(40)°.

Table 2. Selected Bond Lengths (Å) and Angles (deg) for **6**·$PhCH_3$ and **7**·$1.5PhCH_3$[a]

bond lengths		bond angles	
		6·$PhCH_3$	
Co(1)···Co(2)	3.2617(5)	Co(1)−O(101)−Co(2)	104.14(11)
Co(1)−O(104)	2.0857(19)	O(106)−Co(1)−O(104)	87.21(7)
Co(1)−O(106)	2.1220(19)	O(106)−Co(1)−N(3)	91.91(8)
Co(1)−O(101)	2.146(3)	O(106)−Co(1)−N(1)	172.77(9)
Co(1)−O(3)	2.257(2)	O(106)−Co(1)−O(3)	88.23(8)
Co(1)−N(3)	2.214(2)	O(104)−Co(1)−N(3)	91.64(8)
Co(1)−N(1)	2.227(2)	O(104)−Co(1)−N(1)	89.63(8)
Co(2)−O(105)	1.988(2)	O(104)−Co(1)−O(3)	174.22(8)
Co(2)−O(103)	2.0910(19)	O(105)−Co(2)−O(103)	90.28(9)
Co(2)−O(101)	1.9876(19)	O(105)−Co(2)−N(5)	91.49(9)
Co(2)−N(5)	2.277(3)	O(105)−Co(2)−N(4)	121.75(10)
Co(2)−N(4)	2.116(2)	O(103)−Co(2)−N(5)	166.95(9)
		O(103)−Co(2)−N(4)	86.60(8)
		7·$1.5PhCH_3$	
Fe(1)···Fe(2)	3.2669(4)	Fe(1)−O(1)−Fe(2)	110.15(7)
Fe(1)−O(1)	1.9572(16)	O(3)−Fe(1)−O(5)	88.70(7)
Fe(1)−O(3)	2.1118(16)	O(3)−Fe(1)−N(3)	88.67(7)
Fe(1)−O(5)	2.0446(16)	O(3)−Fe(1)−N(4)	169.39(7)
Fe(1)−N(3)	2.196(2)	O(5)−Fe(1)−N(3)	100.68(7)
Fe(1)−N(4)	2.259(2)	O(5)−Fe(1)−N(4)	90.78(8)
Fe(2)−O(1)	2.0270(15)	O(4)−Fe(2)−O(6)	87.19(6)
Fe(2)−O(4)	2.1091(15)	O(4)−Fe(2)−O(7)	175.50(6)
Fe(2)−O(6)	2.1394(15)	O(4)−Fe(2)−N(1)	93.64(7)
Fe(2)−O(7)	2.2917(18)	O(4)−Fe(2)−N(2)	87.56(7)
Fe(2)−N(1)	2.2236(19)	O(6)−Fe(2)−N(1)	89.02(6)
Fe(2)−N(2)	2.2594(19)	O(6)−Fe(2)−N(2)	168.85(7)

[a] Numbers in parentheses are estimated standard deviations of the last significant figure. Atoms are labeled as indicated in Figures 3 and 4.

Structural Studies of the Diiron Compounds with the Ligand DPE. X-ray quality crystals of **7**·$1.5PhCH_3$ were grown from a toluene solution exposed to pentane by vapor diffusion. The structure of **7** is similar to that of **5** and **6** in that the two metal ions are bridged by two carboxylates and one hydroxide ligand and chelated by two nitrogen atoms, this time from the ligand DPE. Figure 4 shows the structure of **7**, and Table 2 lists selected bond lengths and angles. One metal center, Fe(1), has a distorted trigonal bipyramidal stereochemistry, whereas Fe(2) is pseudooctahedral as a result of coordination of a triflate molecule. The Fe···Fe separation is 3.2669(4) Å, and the Fe−O(H)−Fe bond angle is 110.15(7)°. The Fe−O(H) distances for the five- and six-coordinate metal centers are 1.957(2) and 2.027(2) Å, respectively, and the Fe−O bond lengths of the carboxylate groups average to 2.1012(8) Å. As was observed with the TMEDA ligands in **5** and **6**, the DPE ligands are also twisted away from each other. The five-coordinate iron center has average Fe−N bond lengths of 2.228(1) Å; the Fe−N distances at the coordinately saturated atom average to 2.242(1) Å. As in the structure of **6**, the shorter M−N distances are those located trans to the bridging hydroxide ligand. The triflate group is bound to Fe(2) with a Fe−O bond length of 2.2917(18) Å. The dihedral angle between the carboxylate planes of 69.81(25)° is similar to that found in the structure of compound **6**.

Complex **8** crystallized from a mixture of THF and pentane. The structure of **8** is displayed in Figure 5, and selected bond lengths and angles are listed in Table 3. The two iron(III) centers are bridged by two carboxylate groups and one oxo unit. Each six-coordinate metal atom is further coordinated by the nitrogen

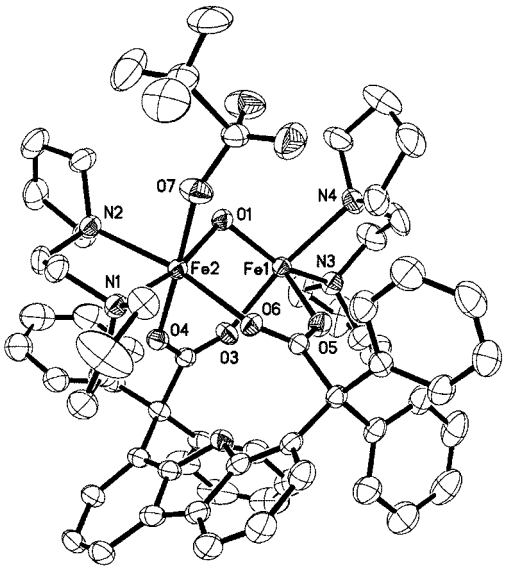

Figure 4. ORTEP diagram of $[Fe_2(\mu\text{-OH})(\mu\text{-Ph}_4\text{DBA})(\text{DPE})_2(\text{OTf})]$ (**7**) showing 50% probability thermal ellipsoids for all non-hydrogen atoms.

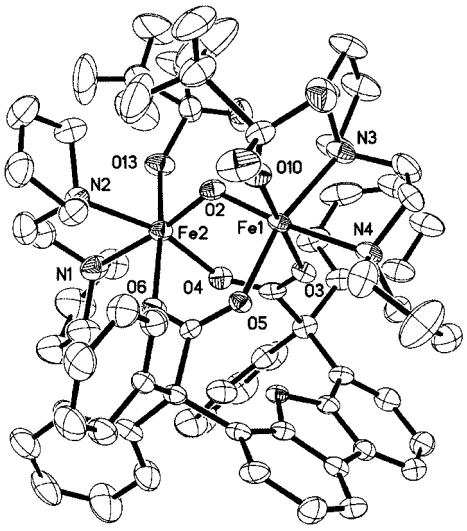

Figure 5. ORTEP diagram of $[Fe_2(\mu\text{-O})(\mu\text{-Ph}_4\text{DBA})(\text{DPE})_2(\text{OTf})_2]$ (**8**) showing 50% probability thermal ellipsoids for all non-hydrogen atoms. For clarity, only one of the disordered triflate ligands is shown (58% occupancy).

atoms of DPE and one terminally bound triflate molecule. The Fe···Fe separation of 3.1310(11) Å and the Fe−O−Fe bond distances of 1.769(4) and 1.774(4) Å are significantly shorter than those in **7**, whereas the Fe−O−Fe bond angle of 124.2(2)° is substantially larger. The Fe−N bond lengths of the two pseudooctahedral metal centers average to 2.197(3) Å. The angle between the carboxylate planes is 79.29(71)°, considerably larger than the corresponding angle found in the structures of compounds **6** and **7**. Coordination of the triflate ligands is stronger than that in **7** as is observed by the shorter Fe−O distances of 2.098(4) and 2.160(4) Å.

UV−Visible Spectroscopic Studies of the Oxygenation of 4, 6, and 7. When O_2 was bubbled through a solution of **4** in CH_2Cl_2 containing 3 equiv of *N*-MeIm at −78 °C, the initially colorless solution rapidly turned red-orange. This oxygenated solution displays two absorption maxima in the optical spectrum, one at 336 nm (∼7300 M^{-1} cm^{-1}) and the other at 470 nm (∼2600 M^{-1} cm^{-1}).[14] The spectrum compares remarkably well with that of oxyHr, the optical bands of which appear at 330 nm (6800 M^{-1} cm^{-1}) and 500 nm (2200 M^{-1} cm^{-1}).[15] The 500 nm band of oxyHr is assigned to a hydroperoxide-to-iron(III) charge-transfer transition,[43] and we attribute the 470 nm band of the model system to the same transition. The low wavelength maximum of this band is consistent with the absence of a (*μ*-1,2-peroxo)diiron(III) unit, because the charge-transfer band for such an adduct generally occurs at or above 600 nm.[39,44] In the absence of *N*-MeIm or in the presence of *N*-methylbenzimidazole or pyridine, oxygenation of **4** at −78 °C also results in absorption changes characteristic of metal-centered oxidations, but the spectra do not resemble that of oxyHr. OxyHr-like spectra are obtained by addition of *N*-benzylimidazole, CH_3CN, or EtCN, however. In addition, a similar spectrum is generated at low temperature by oxygenation of **4** in THF containing 3 equiv of *N*-MeIm or in neat EtCN. These results suggest that a small nitrogen-donor ligand must coordinate to one iron atom in order to form the hydroperoxide-bound adduct. *N*-Methylbenzimidazole is too large to fit into the coordination sphere because of its methyl substituent, and the larger six-membered ring of pyridine may similarly prevent its coordination. As evidenced by monitoring the absorption maximum of the 466 nm band, the dioxygen adduct fully forms within 5 min and begins to decompose after ∼10 min at −78 °C. A product of thermal decomposition of this solution is the tetranuclear iron(III) cluster $[Fe_4(\mu_3\text{-O})(\mu\text{-O})(\mu\text{-OH})_2(\mu\text{-Ph}_4\text{DBA})_2(\text{TMEDA})_3](\text{OTF})_2$, in which the remnants of two molecules of **4** are clearly evident. This cluster was studied by X-ray crystallography, but a complete structural analysis was hindered by poor data quality and severe disorder of the solvent and triflate molecules in the lattice. The core structure of the tetranuclear cation, sketched in Figure 6, differs from that of other tetrairon(III) carboxylate complexes.[45,46]

Table 3. Selected Bond Lengths (Å) and Angles (deg) for **8**·0.5THF·0.25C_5H_{12}[a]

bond lengths		bond angles	
Fe(1)···Fe(2)	3.1310(11)	Fe(1)−O(2)−Fe(2)	124.2(2)
Fe(1)−O(3)	2.033(4)	O(3)−Fe(1)−O(5)	86.33(14)
Fe(1)−O(2)	1.769(4)	O(3)−Fe(1)−O(10)	173.00(15)
Fe(1)−O(5)	2.002(3)	O(3)−Fe(1)−N(3)	88.39(16)
Fe(1)−O(10)	2.160(4)	O(3)−Fe(1)−N(4)	89.37(16)
Fe(1)−N(3)	2.148(5)	O(5)−Fe(1)−N(3)	165.84(18)
Fe(1)−N(4)	2.234(5)	O(5)−Fe(1)−N(4)	86.03(16)
Fe(2)−O(4)	2.037(4)	O(4)−Fe(2)−O(6)	84.64(15)
Fe(2)−O(6)	2.067(4)	O(4)−Fe(2)−N(2)	164.10(17)
Fe(2)−O(2)	1.774(4)	O(4)−Fe(2)−N(1)	85.83(18)
Fe(2)−O(13)	2.098(4)	O(6)−Fe(2)−O(13)	170.60(16)
Fe(2)−N(1)	2.232(5)	O(6)−Fe(2)−N(1)	90.06(17)
Fe(2)−N(2)	2.172(5)	O(6)−Fe(2)−N(2)	87.00(17)

[a] Numbers in parentheses are estimated standard deviations of the last significant figure. Atoms are labeled as indicated in Figure 5.

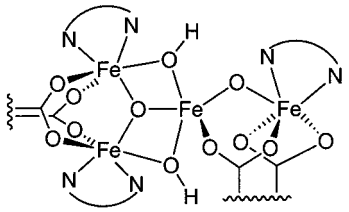

Figure 6. Schematic representation of the cation core of the complex $[Fe_4(\mu_3\text{-O})(\mu\text{-O})(\mu\text{-OH})_2(\mu\text{-Ph}_4\text{DBA})_2(\text{TMEDA})_3](\text{OTf})_2$.

(43) Reem, R. C.; McCormick, J. M.; Richardson, D. E.; Devlin, F. J.; Stephens, P. J.; Musselman, R. L.; Solomon, E. I. *J. Am. Chem. Soc.* **1989**, *111*, 4688−4704.
(44) Kim, K.; Lippard, S. J. *J. Am. Chem. Soc.* **1996**, *118*, 4914−4915.
(45) Gorun, S. M.; Lippard, S. J. *Inorg. Chem.* **1988**, *27*, 149−156.

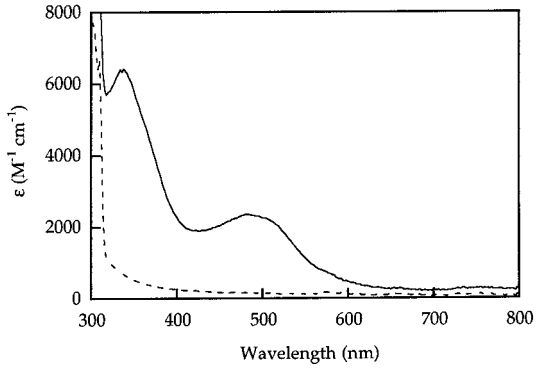

Figure 7. Optical spectra of $[Fe_2(\mu\text{-OH})(\mu\text{-Ph}_4\text{DBA})(\text{DPE})_2(\text{OTf})]$ (**7**) in EtCN at −78 °C before (- - -) and after (−) addition of dioxygen.

The instability of the dioxygen adduct of **4**, even at low temperature, prevented us from determining its structure by X-ray diffraction, and we therefore turned our attention to the preparation of its cobalt analogue. Like the diiron(II) compounds, **6** has an open coordination site to which a potential ligand such as O_2 can bind. Vigorous bubbling of O_2 into a solution of **6** in CH_2Cl_2 at room temperature over several hours did not effect any spectral changes, and the only products that could be characterized from this reaction were dicobalt(II) compounds.

Because **6** did not provide us with the desired structural information, we attempted to increase the stability and hence the lifetime of the diiron(III) hydroperoxide species. The formation of a tetranuclear complex from **4** suggested that the instability of its dioxygen adduct might, in part, be due to the propensity of the TMEDA ligands to dissociate from iron(III). To overcome this problem, we employed an alternative bidentate auxiliary ligand, DPE, to prepare compound **7**.[47] Oxygenation of **7** in neat EtCN yielded an optical spectrum, shown in Figure 7, similar to that of **4**. Absorption maxima were seen at 334 (∼6400 M^{-1} cm^{-1}) and 484 nm (∼2350 M^{-1} cm^{-1}). A similar spectrum is obtained upon oxygenation of **7** in a solution of CH_2Cl_2 or THF containing 3 equiv of *N*-MeIm. Again, the location and intensity of these optical bands strongly resemble those of oxyHr[15] and suggest the formation of a bound hydroperoxide unit. This species is more stable than the corresponding dioxygen-bound adduct of **4**, as noted by the slower decrease with time of the absorption maximum at 484 nm. The O_2-bound adduct is fully formed within 2 min, and essentially no change of the optical band occurs for ∼20 min, after which time the absorbance begins to decrease but at a much slower rate than for the corresponding O_2-adduct of **4**. Clearly, substitution of the TMEDA ligand by DPE does increase the stability of the hydroperoxide species but not enough for us to isolate the adduct in a form suitable for study by X-ray crystallography.

Mössbauer Spectroscopy. The 4.2 K Mössbauer spectrum of solid **4**, shown in Figure 8A, reveals a slightly asymmetric signal. The data were fit to a single quadrupole doublet with δ = 1.21(2) mm s^{-1} and ΔE_Q = 2.87(2) mm s^{-1}, and these extracted parameters fit very well with those of deoxyHr (δ = 1.20, ΔE_Q = 2.89 mm s^{-1}).[48] Although the solid-state molecular structure of **4** clearly shows that the two iron sites have distinct

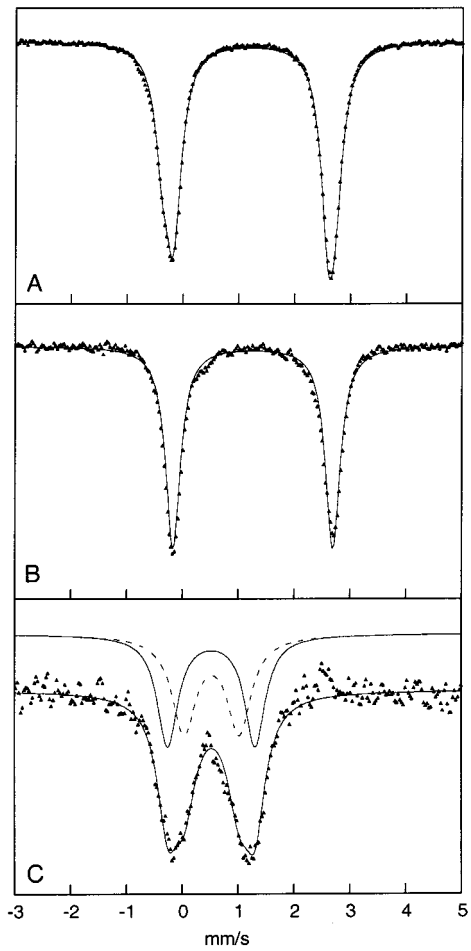

Figure 8. Mössbauer spectra at 4.2 K of (A) $[Fe_2(\mu\text{-OH})(\mu\text{-Ph}_4\text{DBA})(\text{TMEDA})_2(\text{OTf})]$ (**4**) as a powdered solid, (B) **4** as a THF frozen solution containing 3 equiv of *N*-MeIm, and (C) **4** + O_2 as a THF frozen solution containing 3 equiv of *N*-MeIm. In the spectra of (A) and (B) and the lower curve of (C), experimental data (▲) and calculated fit (−) are shown. The upper curves of (C) show two subsets for the calculated spectra of **4** + O_2.

coordination environments, this asymmetry is not reflected on the Mössbauer time scale. Similarly, the frozen THF solution Mössbauer spectrum of **4** in the presence of 3 equiv of *N*-MeIm reveals a single doublet with δ = 1.26(2) mm s^{-1} and ΔE_Q = 2.86(2) mm s^{-1} (Figure 8B). Because these extracted parameters match well those of solid **4**, we conclude that the (μ-hydroxo)diiron(II) core is retained in solution.

The addition of O_2 to a solution of **4** in THF with 3 equiv of *N*-MeIm resulted in average shifts of δ to 0.53(1) mm s^{-1} and ΔE_Q to 1.28(3) mm s^{-1}. The spectrum is shown in Figure 8C. These parameters correlate reasonably well with those of oxyHr ($\delta_{av} \approx 0.53$, $\Delta E_{Qav} \approx 1.51$ mm s^{-1})[48] and indicate that the oxygen-bound adduct of **4** contains a (μ-oxo)diiron(III) core.

Mössbauer spectra were also recorded for the DPE derivative **7** (Figure 9). The solid-state spectrum was fit best as two quadrupole doublets. The data were fit equally well with either the same isomer shift (Figure 9A) or the same quadrupole splitting (Figure 9B), and therefore, we report both fits (for same δ, δ_1 = 1.23(2), ΔE_{Q1} = 2.62(2), δ_2 = 1.22(2), ΔE_{Q2} = 2.99(2) mm s^{-1}; for same ΔE_Q, δ_1 = 1.15(2), ΔE_{Q1} = 2.78(2) mm s^{-1}, δ_2 = 1.32(2), ΔE_{Q2} = 2.78(2) mm s^{-1}). The extracted parameters are in good agreement with those of deoxyHr.[48] The Mössbauer spectrum of **7** in EtCN as a frozen solution revealed a doublet with an isomer shift and quadrupole splitting almost identical to that of solid-state **7**, indicating the retention of the

(46) Armstrong, W. H.; Roth, M. E.; Lippard, S. J. *J. Am. Chem. Soc.* **1987**, *109*, 6318−6326.
(47) Remenar, J. F.; Lucht, B. L.; Kruglyak, D.; Romesberg, F. E.; Gilchirst, J. H.; Collum, D. B. *J. Org. Chem.* **1997**, *62*, 5748−5754.
(48) Okamura, M. Y.; Klotz, I. M.; Johnson, C. E.; Winter, M. R. C.; Williams, R. J. P. *Biochemistry* **1969**, *8*, 1951−1958.

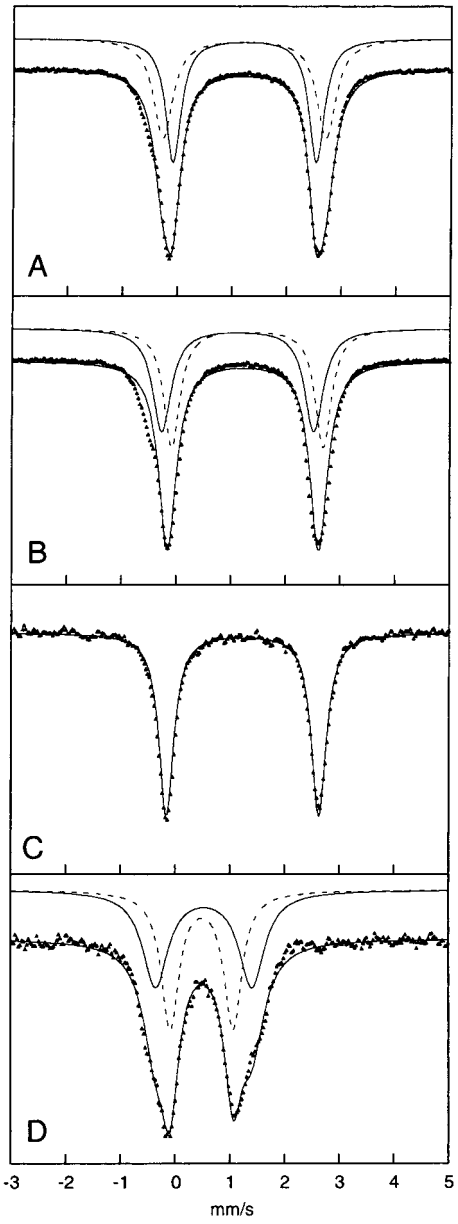

Figure 9. Mössbauer spectra at 4.2 K of $[Fe_2(\mu\text{-OH})(\mu\text{-Ph}_4\text{DBA})(\text{DPE})_2(\text{OTf})]$ (**7**) as a powdered solid with (A) same isomer shift and (B) same quadrupole splitting fits and of frozen EtCN solutions of **7** (C) without O_2 and (D) with O_2. In the spectra of (C) and the lower curves of (A), (B), and (D), experimental data (▲) and calculated fit (−) are shown. The upper curves of (A), (B), and (D) show two subsets for the calculated spectra.

hydroxide-bridged diiron(II) core in solution (Figure 9C). Oxygenation of **7** in EtCN resulted in a spectrum, shown in Figure 9D, that was fit as two overlapping quadrupole doublets ($\delta_{av} = 0.51(1)$, $\Delta E_{Qav} = 1.46(3)$ mm s^{-1}). The similarity of the extracted parameters with those of oxyHr indicates that reaction of dioxygen and **7** in EtCN forms an oxo-bridge diiron(III) core. A summary of Mössbauer parameters for both **4** and **7** is provided in Table 4.

Resonance Raman Spectroscopy. In our earlier communication detailing the reaction of complex **4** with dioxygen, we reported resonance-enhanced Raman bands for the O−O stretch[14] at 843 cm^{-1} ($^{16}O_2$) and 797 cm^{-1} ($^{18}O_2$) that match well with those of oxyHr,[49] suggesting the presence of a terminally bound hydroperoxide unit. To obtain additional evidence regarding the binding mode of the proposed peroxide ligand, we employed a statistical mixture of ^{16}O- and ^{18}O-labeled dioxygen (25% $^{16}O_2$, 25% $^{18}O_2$, 50% $^{16}O^{18}O$) in the low-temperature oxygenation of compound **7**. The use of unsymmetrically labeled dioxygen is ideal for discriminating between symmetric μ-1,2-peroxo and the terminally coordinated hydroperoxide binding modes for oxyHr.[49] Specifically, three absorptions with peak heights and area ratios of 1:2:1 are expected for a symmetrical binding mode, whereas four peaks with equal ratios should arise from an unsymmetrical peroxide coordination.

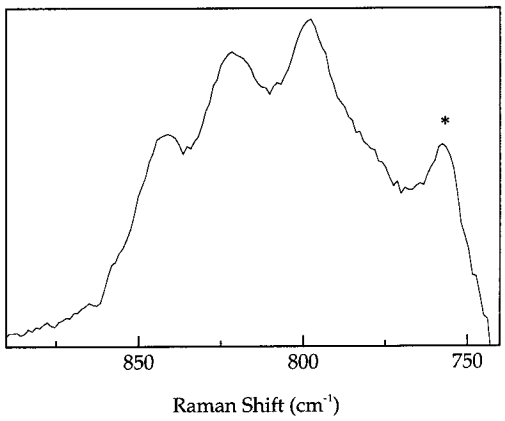

Figure 10. Resonance Raman difference spectrum of $[Fe_2(\mu\text{-OH})(\mu\text{-Ph}_4\text{DBA})(\text{DPE})_2(\text{OTf})]$ (**7**) in CH_2Cl_2 containing 1% CH_3CN after oxygenation with a statistical mixture of ^{16}O- and ^{18}O-labeled dioxygen. The asterisk (∗) denotes an artifact arising from subtraction of the reduced and oxidized samples.

Table 4. Summary of Mössbauer Parameters for **4** and **7** Recorded at 4.2 K (mm s^{-1})

complex	δ	ΔE_Q	Γ
4 (powder)	1.21(2)	2.87(2)	0.34(2)
4 (THF, 3 equiv of *N*-MeIm)	1.26(2)	2.86(2)	0.32(2)
4 + O_2 (THF, 3 equiv of *N*-MeIm)	0.53(2)	0.99(9)	0.52(9)
	0.53(2)	1.57(9)	0.45(9)
7 (powder), same δ	1.23(2)	2.62(2)	0.34(2)
	1.22(2)	2.99(2)	0.43(2)
7 (powder), same ΔE_Q	1.15(2)	2.78(2)	0.42(2)
	1.32(2)	2.78(2)	0.32(2)
7 (EtCN)	1.23(2)	2.79(2)	0.33(2)
7 + O_2 (EtCN)	0.53(2)	1.76(9)	0.56(9)
	0.49(2)	1.15(9)	0.39(9)

The published resonance Raman spectrum of oxyHr using a mixture of ^{16}O- and ^{18}O-labeled dioxygen displays three peaks, the central one of which was broader than the other two and had a flattened top.[49] This broad peak (822 cm^{-1}) was deconvoluted into two separate features at 825 cm^{-1} (Fe−^{16}O−^{18}O) and 819 cm^{-1} (Fe−^{18}O−^{16}O).[49] When we carried out the low-temperature reaction of complex **7** with the statistical mixture of dioxygen in CH_2Cl_2 containing 1% CH_3CN, we recorded three resonance-enhanced bands in the Raman spectrum at 841, 822, and 798 cm^{-1} (Figure 10). We attribute the 841 cm^{-1} band to the O−O stretch of $^{16}O_2$ and the 798 cm^{-1} to the O−O stretch of $^{18}O_2$.[14] The peak at 822 cm^{-1} appears to have a slightly greater half-width than the other two. The baseline of the spectrum is ill-defined, however, being close to a strong solvent absorption. This property prevented us from separating the 822 cm^{-1} band into two closely spaced features in order to provide conclusive evidence for a terminally bound hydroperoxide unit.

EPR and ENDOR Spectroscopy. It is well-documented that the one-electron reduction of diiron(III) sites of proteins, enzymes, and inorganic compounds can be achieved by irradia-

(49) Klotz, I. M.; Kurtz, D. M., Jr. *Acc. Chem. Res.* **1984**, *17*, 16−22.

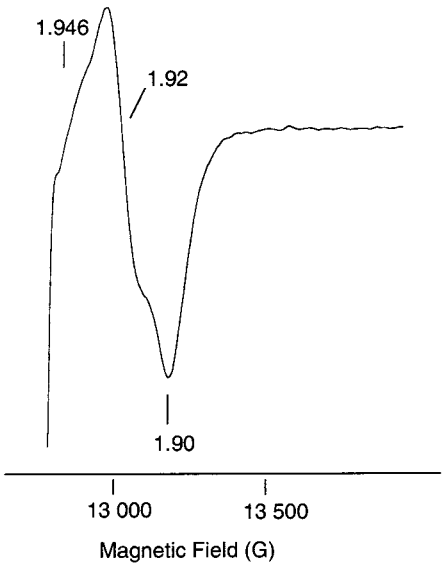

Figure 11. 35.1 GHz EPR spectrum of the cryogenically reduced dioxygen adduct of [Fe_2(μ-OH)(μ-Ph_4DBA)(DPE)$_2$(OTf)] (**7**) at 2 K in 2:1 2-MeTHF/EtCN. Instrument conditions were as follows: modulation frequency 100 kHz, modulation amplitude 1.3 G, MW power 0.5 mW.

tion with γ-rays in frozen solutions at liquid nitrogen temperatures.[27,50] The cryogenically generated diiron(II,III) complex retains the original structure of the diiron(III) compound and can provide insight to the structure of the diiron(III) species following EPR and ENDOR spectroscopic studies.[28,50] The product of the reaction of complex **7** in 2:1 2-MeTHF/EtCN with dioxygen at −78 °C shows no EPR spectrum at 2 K. Upon cryogenic reduction at 77 K, a rhombic EPR spectrum with g = 1.90, 1.92, and ∼1.946 (Figure 11) is observed. This spectrum is characteristic of oxo-bridged diiron(II,III) cores and is consistent with our other spectroscopic evidence for proton transfer coupled with metal-based oxidation. In addition, this spectrum is similar to that of cryoreduced oxyHr (g = 1.90, 1.92).[51]

The 2 K ^{1}H ENDOR spectra of the dioxygen adduct of **7**, acquired at g = 1.90 and 1.92, display a weak doublet with A ∼11.5 MHz that we tentatively assign to the proton of the putative hydroperoxide ligand (Figure 12, solid line). The corresponding spectrum of cryoreduced oxyHr shows peaks at 9.5 MHz.[51] The ^{1}H ENDOR spectrum, however, is not well-resolved, which we attribute to spin-relaxation problems caused by the presence of the terminal hydroperoxide ligand. To assign more definitively the doublet, we prepared the chemically oxidized analogue **8**, the coordination sphere of which is very similar to that of the O_2-adduct of **7**, the only difference being the substitution of the hydroperoxide ligand by a bound triflate molecule. The corresponding ENDOR spectrum of **8** lacks the A ∼11.5 MHz doublet (Figure 12, broken line), supporting our assignment of the signal as arising from the proton of the hydroperoxide ligand.

X-ray Absorption Spectroscopy. The Fe K-edge and preedge (1s → 3d transitions) for **7** are consistent in shape and energy with previously measured data for Fe(II) complexes. The preedge contains at least three low-intensity transitions centered at ∼7111.5, 7112, and 7113.5 eV (Figure 13). Similar sets of transitions have been observed for high-spin ferrous complexes

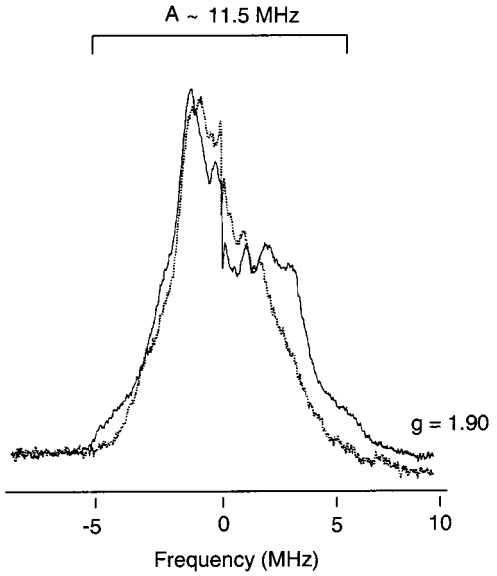

Figure 12. ^{1}H ENDOR spectra of the cryogenically reduced dioxygen adduct of [Fe_2(μ-OH)(μ-Ph_4DBA)(DPE)$_2$(OTf)] (**7**) (−) and cryogenically reduced [Fe_2(μ-O)(μ-Ph_4DBA)(DPE)$_2$(OTf)$_2$] (**8**) (···) in 2:1 2-MeTHF/EtCN at 2 K.

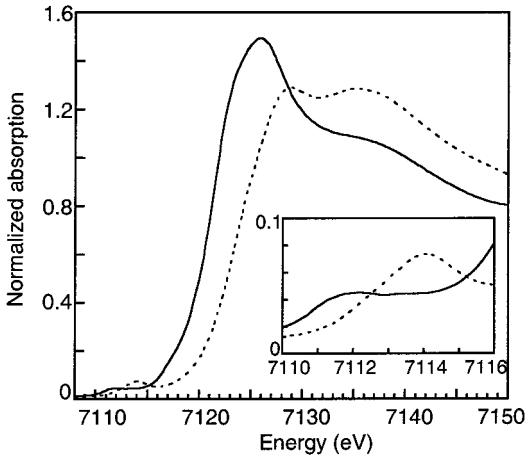

Figure 13. Fe K-edges and preedges (1s → 3d transitions) for [Fe_2(μ-OH)(μ-Ph_4DBA)(DPE)$_2$(OTf)] (**7**) (−) and its O_2-adduct (- - -). Preedge transitions are shown in the inset.

with approximately octahedral geometry.[52] The shape and overall higher energy of the K-edge for the O_2 adduct of **7**, also shown in Figure 13, indicate that both iron centers have been oxidized to Fe(III). The preedge region for the oxidized species contains an intense peak at ∼7114 eV and a much weaker shoulder at ∼7112.5 eV (Figure 13, inset). This pattern of energies and intensities is highly characteristic of (μ-oxo)-diiron(III) complexes and is distinct from patterns observed for compounds containing a (μ-hydroxo)diiron(III) core.[52]

The best fit to EXAFS for the O_2-adduct of **7** (Figure 14) yields an average first coordination shell Fe−ligand distance of 2.06 Å (Table 5, fit 8), a contraction that is consistent with oxidation of the iron centers to Fe(III). There is a dramatic improvement in the fit upon inclusion of a short first coordination shell component, namely one O/N ligand per iron at 1.79 Å (Table 5, fits 1 and 2). This component is consistent with an oxide ligand bound to each iron(III) center. Together with the distinctive preedge for the complex, it is strongly suggestive of

(50) Davydov, R.; Kuprin, S.; Gräslund, A.; Ehrenberg, A. *J. Am. Chem. Soc.* **1994**, *116*, 11120−11128.
(51) Davydov, R. Unpublished results.
(52) Westre, T. E.; Kennepohl, P.; DeWitt, J. G.; Hedman, B.; Hodgson, K. O.; Solomon, E. I. *J. Am. Chem. Soc.* **1997**, *119*, 6297−6314.

Table 5. Results of Fits 1−8 to EXAFS Data for O_2-adduct of [Fe_2(μ-OH)(μ-Ph_4DBA)(DPE)$_2$(OTf)] (**7**) in EtCN[a]

absorber−scatterer	1	2	3	4	5	6	7	8[b]
Fe−O/N	6.0, 2.11 (0.022)	1.0, 1.79 (0.004)	1.0, 1.79 (0.002)	1.0, 1.78 (0.002)	1.0, 1.78 (0.002)	1.0, 1.78 (0.001)	1.0, 1.79 (0.002)	1.0, 1.79 (0.002)
Fe−O/N		5.0, 2.13 (0.010)	2.0, 2.01 (0.003)	2.0, 1.99 (0.004)	2.0, 2.00 (0.004)	2.0, 2.00 (0.004)	2.0, 2.01 (0.004)	2.0, 2.01 (0.004)
Fe−O/N			3.0, 2.17 (0.003)	3.0, 2.16 (0.004)	3.0, 2.16 (0.004)	3.0, 2.16 (0.004)	3.0, 2.18 (0.004)	3.0, 2.18 (0.004)
Fe−Fe				1.0, 3.01 (0.016)	1.0, 2.96 (0.006)	1.0, 3.14 (0.005)	1.0, 2.97 (0.006)	1.0, 3.16 (0.004)
Fe−C					4.0, 3.17 (0.003)	4.0, 2.97 (0.002)	4.0, 3.18 (0.002)	4.0, 3.00 (0.002)
Fe−C							2.0, 4.06 (0.007)	2.0, 4.06 (0.007)
Fe−C							3.0, 4.58 (0.006)	3.0, 4.58 (0.006)
E_0 (eV)	7023.6	7023.4	7019.8	7018.9	7020.0	7019.9	7022.5	7022.2
R[c]	0.844	0.5481	0.5277	0.4569	0.3539	0.3078	0.3341	0.2703

[a] First number is the number of equivalent backscattering atoms, second number is the absorber−scatterer distance (Å), and number in parentheses is the Debye−Waller factor, σ^2 (Å^2). [b] Best fit. [c] R is a goodness-of-fit parameter, where $R = [\sum k^6(\chi_{obs} - \chi_{calc})^2/N]^{1/2}$ (N = number of points in EXAFS spectrum), $R = R^2/[(2\Delta k \Delta R/\pi) -$ no. variables in fit]. The errors in the distances are in the range of ±0.02 Å.[54]

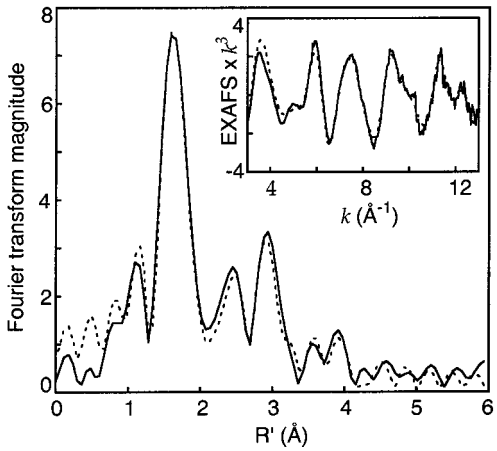

Figure 14. EXAFS data (inset) and their Fourier transform (non-phase-shift-corrected) for the O_2-adduct of [Fe_2(μ-OH)(μ-Ph_4DBA)(DPE)$_2$-(OTf)] (**7**). Data (−) and best fits to the data (- - -) are shown.

a (μ-oxo)diiron(III) unit in the complex. The best fit for the EXAFS (Table 5, fit 8) models each iron center as six-coordinate with one O/N scatterer at 1.79 Å, two at 2.01 Å, and three at 2.18 Å. These distances are consistent with expected bond lengths for oxide, carboxylate, and amine/hydroperoxide ligands, respectively, in a ferric complex. Fits to outer-shell components in the EXAFS demonstrate considerable interference between Fe···Fe and Fe···C scattering contributions, as is often observed for diferric complexes. Inclusion of two outer-shell distances of ∼3 and 3.15 Å, modeled as either Fe···Fe or Fe···C scattering, greatly improves the fit (Table 5, fits 5 and 6), with Fe···Fe as the longer distance consistently giving significantly lower fit functions. The Fourier transform features at longer distances represent contributions from many Fe−C (pyrrole, phenyl, tertiary carbons) interactions in certain distance ranges and were modeled as two average-distance Fe−C waves around 4.1 and 4.6 Å.

As shown by both EXAFS[53] and X-ray crystallography,[5] oxyHr contains a μ-oxo ligand with average Fe−O distances of 1.82 and 1.83 Å, as determined by the two techniques, respectively. One of the iron(III) centers has a bound hydroperoxide with a Fe(III)−O(OH) distance of 2.15 Å, as determined by X-ray crystallography; this value is close to the average 2.18 Å Fe−O/N distance found for the model dioxygen adduct, although it is not possible to associate this distance specifically with an Fe(III)−OO(H) interaction in the model. The major differences between the model and protein are in the remaining first coordination shell distances and in the Fe···Fe separation. Compound **7** is very similar in structure and ligand types to deoxyHr. Upon oxygenation, however, the average Fe−ligand distance in the model contracts from ∼2.14 to ∼2.06 Å, whereas the equivalent distance in the protein undergoes a smaller change, as determined by X-ray crystallography (∼2.17 to ∼2.13 Å) and EXAFS (∼2.15 to ∼2.11 Å). Furthermore, the Fe···Fe separation in **7** is 3.12 Å; upon oxygenation, this distance does not change much (3.14 Å), but a small collapse in Fe···Fe separation occurs upon oxygenation of the protein, changing from 3.32 to 3.27 Å and 3.57 to 3.24 Å, as determined by X-ray crystallography and EXAFS,[54] respectively. The shorter average Fe(III)−ligand and Fe···Fe distances in the model system may arise because our small-molecule compound does not incorporate any interactions with the secondary coordination sphere, whereas there are numerous such interactions in the protein.

Conclusions. Two diiron complexes, [Fe_2(μ-OH)(μ-Ph_4DBA)-(TMEDA)$_2$(OTf)] (**4**) and [Fe_2(μ-OH)(μ-Ph_4DBA)(DPE)$_2$(OTf)] (**7**), were prepared and studied as functionally relevant small molecule mimics of the Hr active site. In the reduced state, **4** and **7** accurately reproduce the asymmetric coordination environment of deoxyHr. Mössbauer spectroscopy also reveals that these complexes have δ and ΔE_Q values similar to those of the reduced protein. Upon oxygenation of these compounds at −78 °C in the presence of a sufficiently small coordinating base or solvent, dioxygen adducts of **4** and **7** are generated and display optical spectra similar to that of oxyHr. Mössbauer, resonance Raman, EPR, ENDOR, and EXAFS spectra of the O_2-adduct of **7** indicate the presence of a (μ-oxo)diiron(III) core. Although it is not possible conclusively to assign a Fe−OOH bond to the adduct, the Fe−ligand bond distances are consistent with those expected for oxide, carboxylate, and amine/hydroperoxide ligands.

Acknowledgment. This work was supported by grants from the National Science Foundation, National Institute of General

(53) Zhang, K.; Stern, E. A.; Ellis, F.; Sanders-Loehr, J.; Shiemke, A. K. *Biochemistry* **1988**, *27*, 7470−7479.

(54) The crystallographically defined Fe···Fe separation is perhaps more reliable for the diferrous protein, given that it is fairly long. For a discussion of EXAFS determination of metal···metal separations, see: Riggs-Gelasco, P. J.; Stemmler, T. L.; Penner-Hahn, J. E. *Coord. Chem. Rev.* **1995**, *144*, 245−286.

Medical Science (Grant GM32134, S.J.L.), and NIH (Grant RR-01209, K.O.H.). T.J.M. thanks the NIH for a postdoctoral fellowship, and J.K. gratefully acknowledges NSERC for funding. B.S. was supported by the Swiss National Science Foundation as a postdoctoral fellow. We thank Dr. A. M. Barrios for performing the resonance Raman experiments and Mr. D. Lee for assistance in the acquisition of Mössbauer spectra and many helpful discussions. Stanford Synchrotron Radiation Laboratory operations are funded by the U.S. Department of Energy. The SSRL Structural Molecular Biology program is supported by the National Institutes of Health, National Center for Research Resources, Biomedical Technology Program, and the DOE Office of Biological and Environmental Research.

Supporting Information Available: The full numbering schemes of compounds **6**−**8** in Figures S1−S3 and X-ray crystallographic files for compounds **6**−**8** in CIF format. This material is available free of charge via the Internet at http://pubs.acs.org.

IC010076B